Journal of Molecular Structure 1138 (2017) 55–63

Contents lists available at ScienceDirect

Journal of Molecular Structure

journal homepage: http://www.elsevier.com/locate/molstruc

New bioactive silver(I) complexes: Synthesis, characterization, anticancer, antibacterial and anticarbonic anhydrase II activities

Ummuhan O. Ozdemir [a, *], Neslihan Ozbek [b], Zuhal Karagoz Genc [c], Firdevs İlbiz [a], Ayla Balaban Gündüzalp [a]

[a] Department of Chemistry, Faculty of Science, Gazi University, Ankara, Turkey
[b] Department of Chemistry, Faculty of Education, Ahi Evran University, Kırşehir, Turkey
[c] Department of Materials Engineering, Faculty of Engineering, Adıyaman University, Adıyaman, Turkey

ARTICLE INFO

Article history:
Received 17 January 2017
Received in revised form
22 February 2017
Accepted 28 February 2017
Available online 6 March 2017

Keywords:
Silver(I) complexes
Alkyl sulfonic acide hydrazide
Anticancer
Antibacterial
Anti carbonic anhydrase II

ABSTRACT

Silver(I) complexes of alkyl sulfonic acide hydrazides were newly synthesized as homologous series. Methanesulfonic acide hydrazide (L1), ethanesulfonic acide hydrazide (L2), propanesulfonic acide hydrazide (L3) and butanesulfonic acide hydrazide (L4) were used for complexation with Ag(I) ions. The silver complexes obtained in the mol ratio of 1:2 have the structural formula as $Ag(L1)_2NO_3$ (**I**), $Ag(L2)_2NO_3$ (**II**), $Ag(L3)_2NO_3$ (**III**), $(Ag(L4)_2NO_3$ (**IV**). The Ag(I) complexes exhibit distorted linear two-fold coordination in $[AgL_2]^+$ cations with uncoordinated nitrates. Ligands are chelated with silver(I) ions through unsubstituted primary nitrogen in hydrazide group. Ag(I) complexes were characterized by using elemental analysis, spectroscopic methods (FT-IR, LC-MS), magnetic susceptibility and conductivity measurements. Silver(I) complexes were optimized using PBEPBE/LanL2DZ/DEF2SV basic set performed by DFT method with the Gaussian 09 program package. The geometrical parameters, frontier molecular orbitals (HOMOs and LUMOs) and molecular electrostatic potential (MEP) mapped surfaces of the optimized geometries were also determined by this quantum set. The anticancer activities of silver(I) complexes on MCF-7 *human breast cancer cell line* were investigated by comparing IC_{50} values. The antibacterial activities of complexes were studied against Gram positive bacteria; *S. aureus* ATCC 6538, *B. subtilis* ATCC 6633, *B. cereus* NRRL-B-3711, *E. faecalis* ATCC 29212 and Gram negative bacteria; *E. coli* ATCC 11230, *P. aeruginosa* ATCC 15442, *K. pneumonia* ATCC 70063 by using disc diffusion method. The inhibition activities of Ag(I) complexes on carbonic anhydrase II enzyme (hCA II) were also investigated by comparing IC_{50} and Ki values. The biological activity screening shows that Ag(I) complex of butanesulfonicacidehydrazide (**IV**) has the highest activity against tested breast cancer cell lines MCF-7, Gram positive/Gram negative bacteria and carbonic anhydrase II (hCA II) isoenzyme.

1. Introduction

Silver complexes were used as antimicrobial agents for many years and now found applications as antiseptics [1–4]. Some of them exhibit significant antiproliferative properties which can be higher than the corresponding activities of cisplatin [5,6]. An additional advantage of using silver coordination compounds in the development of new metallotherapeutic drugs is their low toxicity to humans. However, this feature also raises the question of whether such compounds, when the proper ligands are present, can display higher antiproliferative activities in cancer cells. The molecules of sulfonic acide hydrazide involve two pharmacophoric fragments: sulfonamide group and hydrazine residue. Lots of them have strong cytostatic [7,8], antibacterial [9] and analgesic activities [10,11], as well as carbonic anhydrase inhibition properties [12]. Sulfonamides are a vital class of antimicrobial agents in the world owing to their low cost and ability to slow bacterial growth in wounds or infected organs without appreciable toxicity to normal tissues. Metal complexes of sulfonamides have received interest in bioinorganic chemistry [13–16]. To find better compounds, some metallo sulfonamides have much attention due to the fact that complexes show more activity than free ligands. For example, Ag(I)–sulfadiazine complex is used for human burn treatment [14,15] and the Zn(II)–sulfadiazine complex is used for prevention

* Corresponding author.
E-mail address: ummuhan@gazi.edu.tr (U.O. Ozdemir).

http://dx.doi.org/10.1016/j.molstruc.2017.02.101
0022-2860/

of bacterial infection in burned animals [16]. The potent anti-inflammatory properties of silver(I) ions are well known as skin wound dressings for the treatment of bacterial infections and recently, silver nanoparticles have been used as antibacterial agents. Ag(I) complexes with various types of ligands containing active sites such as nitrogen, oxygen, phosphorus or sulfur etc. have been studied for their antitumor activities. Moreover, the selectivity towards cancer cells could be achieved using appropriate ligands coordinating with silver(I) ions [17].

Since the number of metal complexes called sulfa drugs has increased, the interaction of metal ions in drugs administered for therapeutic reasons has became a subject of importance. Due to sulfonamides/sulfonylhydrazines/sulfonylhydrazones and their metal complexes have significant pharmacologic applications and widespread use in medicine, these compounds gain importance in bioinorganic and metal based drug chemistry.

In our previous studies, we reported the antibacterial and cytotoxic effect of methane sulfonic acid hydrazide (CH_3SO_2-$NHNH_2$) and its sulfonylhydrazone derivatives [18,19], as well as its metal complexes [20–22]. Ethane and prophane sulfonylhydrazone derivatives and their transition metal complexes were synthesized and screened for their antimicrobial activities [23–26]. Furthermore, ethanesulfonylhydrazone/prophanesulfonylhydrazone derivatives and their transition metal complexes and also different aromatic/heteroaromatic sulfonylhydrazone derivatives were investigated for their inhibitory effects on carbonic anhydrase II (hCA II) isoenzyme [25,27]. In addition, alkyl (Alkyl: methane, ethane, prophane, buthane, **L1-L4**) and acetyl sulfonic acid hydrazide derivatives were synthesized for biological studies. The structure of ligands were reported in our previous work [18,28].

As part of ongoing studies, alkyl sulfonic acide hydrazide-Ag(I) complexes (**I**–**IV)** were synthesized for the first time and characterized by using elemental analysis, FT-IR, LC–MS, magnetic susceptibility and conductivity measurements. Theoretical calculations invoking structural optimization, geometrical parameters (bond lenghts and bond angles), electronic properties (frontier molecular orbital (FMO) energies and molecular electrostatic potential (MEP) mapped surfaces) were performed using DFT/PBEPBE method with LanL2DZ/DEF2SV basis set in Gaussian 09 program. The anticancer activities of silver(I) complexes towards MCF-7 human breast cancer cell line were investigated by comparing IC_{50} values. The antibacterial activities of synthesized complexes were studied against Gram positive bacteria; *S. aureus* ATCC 6538, *B. subtilis* ATCC 6633, *B. cereus* NRRL-B-3711, *E. faecalis* ATCC 29212 and Gram negative bacteria; *E. coli* ATCC 11230, *P. aeruginosa* ATCC 15442, *K. pneumonia* ATCC 70063 by using disc diffusion method and compared with Standard antibiotics. The inhibition activities on carbonic anhydrase II enzyme (hCA II) were also evaluated by comparing IC_{50} (IC_{50} represents the molarity of inhibition as 50% decrease of enzyme activity) and K_i (inhibitor–enzyme dissociation constant) values.

2. Experimental

2.1. Physical measurements

The solvents were purified and distilled according to routine procedures. Methane/ethane/prophane and butane sulfonyl chloride, hydrazine hydrate, silver(I) nitrate were commercial products (purum). Elemental analyses were performed according to standard micro analytical procedures by Leco CHNS-932. The infrared spectra of the compounds as KBr-disks were recorded in the range of 4000-400 cm^{-1} with a Mattson 1000 FT-IR spectrometer. UV–Vis spectra were recorded on UNICAM-UV 2-100 spectrophotometer. LC-MS spectra were recorded on LCT Premier XE UPLC/MS-TOF spectrophotometer. Melting points of silver complexes were determined with a Gallenkamp melting point apparatus. The molar magnetic susceptibilities were measured on powdered samples using Gouy method. The molar conductance measurements were carried out using a Siemens WPA CM 35 conductometer. The anticancer activities of Ag(I) complexes on MCF-7 *human* breast cancer cell line were investigated by MTT assay method. The cell cultures were incubated under 5% CO_2/air at 37 °C conditions in Nuaire humidified carbon dioxide incubator (Plymouth, MN, USA). Cells' state was controlled by inverted microscope (Soif Optical Inc. China) and results are expressed as Mean ± STD. Statistical analysis and comparison between mean values for cytotoxicity were performed by Tukey variance analysis (SPSS 10.0 for Windows; Chicago, IL, USA). The disc diffusion method was used to determine the antibacterial activities of complexes against Gram positive bacteria; *S. aureus* ATCC 6538, *B. subtilis* ATCC 6633, *B. cereus* NRRL-B-3711, *E. faecalis* ATCC 29212 and Gram negative bacteria; *E. coli* ATCC 11230, *P. aeruginosa* ATCC 15442, *K. pneumonia* ATCC 70063. Bacterial cultures were obtained from Gazi University, Biology Department in Turkey. The inhibition activities of synthesized complexes against carbonic anhydrase II (hCA II) were investigated by comparing K_i and IC_{50} values.

2.2. General procedure for the synthesis of Ag(I) complexes

The reactions of silver(I) nitrate with various alkyl sulfonic acide hydrazides (alkyl, R:methan, ethane, prophane, butane) were carried out as follows [17]: An acetonitrile solution of the alkyl sulfonic acide hydrazides, R-SO_2NHNH_2 (1.2 mmol) was added dropwise into the solution of methanol/acetonitrile (25 mL) of $AgNO_3$ (0.6 mmol). The reaction mixture was heated under reflux for 1 day at 50 °C and left in deep freze for 5 h. The solid complexes was collected by filtration, washed with a small volume of acetonitrile/methanol/ether, left in glass oven at 170 °C for a 2 h in vacuo to prevent the hydration and dried in a desiccator over $CaCl_2$.

2.3. Computational section

All quantum chemical calculations for Ag(I)-alkyl sulfonic acide hydrazides were performed by PBEPBE method with LanL2DZ/DEF2SV basic set using DFT in Gaussian 09 software program [29,30]. The geometries of silver(I) complexes were optimized by minimizing energies with respect to geometrical parameters (bond lenghts and bond angles) [31], the frontier molecular orbital energies (HOMO-2, HOMO-1, HOMO and LUMO, LUMO+1, LUMO+2). The molecular electrostatic potential (MEP) mapped surfaces of the optimized geometries were also computed by this quantum set. The different values of the electrostatic potential at the surface are represented by different colours. The positive regions (blue) may be regarded as electrophilic centers whereas the negative regions (red) as nucleophilic sites [32,33].

2.4. Biological activities

2.4.1. Cell culture and cytotoxicity determination

The anticancer activities of Ag(I) complexes on MCF-7 human breast cancer cell line were investigated by MTT assay method. The colorimetric cell viability assay under usage of the tetrazole 3-(4,5-dimethylthiazol-2yl)-2,5-diphenyltetrazolium bromide (MTT) was used to evaluate the cytotoxic effects of the test compounds [34]. MCF-7 cancer cell line were grown as monolayer culture in a high glucose concentration (4.5 g/L) DMEM medium supplemented with 10% fetal calf serum (FCS), 1% L-glutamine (200 mM), 1% of mixture penicillin (100 IU/ml) and streptomycin (100 lg/ml) incubated at 37 °C in atmosphere of 5% CO_2–95% air mixture. Briefly, 5×10^4

Table 1
Analytical and physical data for silver(I) complexes.

Complex	Empirical Formula (Formula Weight)	m.p. (°C)	Yield (%)	Found (Calculated)			
				%C	%H	%N	%S
I	$C_2H_{12}N_5O_7S_2Ag$ 389.87 g/mol	110–1121	50	6,38 (6,16)	3,17 (3,08)	17,63 (17,96)	16,21 (16,42)
II	$C_4H_{16}N_5O_7S_2Ag$ 417.97 g/mol	121–123	40	10,93 (11,40)	3,50 (3,83)	16,28 (16.75)	14,92 (15,32)
III	$C_6H_{20}N_5O_7S_2Ag$ 445.87 g/mol	104–106	55	15,08 (16.15)	4,24 (4.49)	14,98 (15,70)	14,28 (14,35)
IV	$C_8H_{24}N_5O_7S_2Ag$ 473.87 g/mol	132–135	45	19,82 (20,26)	5,04 (5,06)	14,70 (14,77)	13,35 (13,51)

MCF-7 tumor cells were plated in triplicate in 96-well flat bottom tissue culture plates and treated with different concentrations of drugs for the time indicated. MTT (0.005 g/mL in phosphate buffer saline) was added to the cell culture and incubated for 4 h at 37 °C in 5% CO_2 humidified incubator. The formazan crystals formed during the reaction of active mitochondria with MTT were dissolved in 100 mL of isopropanol and readings were taken in a microtiter plate reader using a 570 nm filter. Cytotoxic activity results were evaluated as the IC_{50} values (in μM) and Docetaxel was used as positive control.

2.4.2. Procedure for antibacterial activities

The antibacterial activities of the Ag(I) complexes with alkyl sulfonic acide hydrazide were in vitro tested against Gram positive bacteria; *S. aureus* ATCC 25923, *B. subtilis* RSKK 244, *B. magaterium* RSKK 5117 and Gram negative bacteria; *S. enteritidis* ATCC 13076, *E. coli* ATCC 11230 by using disc diffusion method. Bacterial strains were cultured over night at 310 K in Nutrient Broth. During the survey, these stock cultures were stored in the dark at 277 K. The inocula of microorganisms were prepared from broth cultures and suspensions were adjusted to 0.5 McFarland standard turbidity.

The Ag(I) complexes with alkyl sulfonic acide hydrazide were dissolved in 20% DMSO to final concentration of 5.0 mg mL^{-1} and sterilized by filtration with 0.45 μm millipore filters. Antimicrobial tests were then carried out by the disc diffusion method using 100 μL of suspension containing 10^8 CFU mL^{-1} bacteria spread on a nutrient agar (NA) medium. The discs (6 mm in diameter) were impregnated with 20 μL of each compound (100 μg/disc) at the concentration of 5.0 mg mL^{-1} and placed on the inoculated agar. DMSO impregnated discs were used as negative control. Sulfamethoxazole (300 μg/disc) and sulfisoxazole (300 μg/disc) antibiotics were used as positive controls to determine the sensitivity of one strain/isolate in each microbial species tested. The inoculated plates of bacterial strain isolates were incubated at 37 °C for 24 h. Antimicrobial activities were evaluated by measuring zone diameters of inhibition against bacterial strains in disc diffusion assay. Each assay was repeated twice. Percentage of inhibition by comparing distance of the compounds to the positive control (Sulfamethoxazole) using the equation below [35].

$$\%\ Inhibition = \left[\frac{diameter\ of\ the\ sample}{diameter\ of\ the\ positive\ control}\right]\cdot 100$$

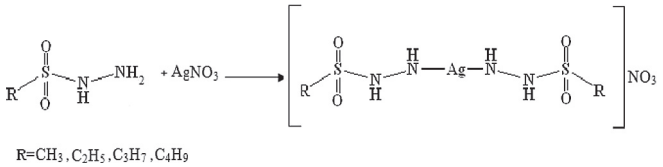

Fig. 1. Preparation of silver(I) complexes with different alkyl sulfonic acid hydrazides (**I**–**IV**).

2.4.3. Procedure for hCA II enzyme inhibitor activities

Carbonic anhydrase II (hCA II) inhibition activities were assayed by the hydrolysis of *p*-nitrophenylacetate to *p*-nitrophenolate [36]. IC_{50} and Ki values of compounds were determined on hCA II isoenzyme. Acetazolamide (5-acetamido-1,3,4-thiadiazole-2-sulfonamide, AAZ) clinically used in hCA II inhibition was investigated as standard inhibitor.

In order to determine IC_{50} values, 100 μL of 3.0 mM *p*-nitrophenylacetate as substrate and four different concentrations (3×10^{-2}, 3×10^{-3}, 5×10^{-4}, 3×10^{-4} M) of inhibitors were used. Reaction was started by adding of 170 μL of 0.05 M tris-SO_4 buffer (pH: 7.6) and 0.1 μL enzyme solution for total volume of 300 μL. The absorbance was determined at 348 nm after 6 min with UV–vis spectrophotometer [37]. This study was repeated three times for each inhibitor. In order to determine IC_{50} values, graphs were drawn using % inhibition values by statistical packing program on a computer. The IC_{50} concentrations of Ag(I)-alkyl sulfonic acide hydrazides were determined from graphs [38]. This method was applied to determine K_i values. In the media with or without inhibitor, the substrate concentrations were taken at 0.3, 0.6, 1.0, 3.0 mM. The Linewear-Burk graphs were obtained and K_i values were calculated according to *Cheng Prusoff equation*.

3. Results and discussion

Analytical data and some physical properties of the Ag(I) complexes of alkyl sulfonic acide hydrazide are summarized in Table 1. The general synthetic route used to prepare the compounds are illustrated in Figs. 1–2. The reaction of corresponding alkyl sulfonic acide hydrazides with silver (I) nitrate was employed to form Ag(I) complexes with methanesulfonicacide hydrazide (**I**), ethanesulfonicacide hydrazide (**II**), propanesulfonicacide hydrazide (**III**) and butanesulfonicacide hydrazide (**IV**). The geometry optimization, geometrical and electronic parameters of silver(I) complexes were performed by using PBEPBE/LanL2DZ/DEF2SV quantum set with DFT method in Gaussian 09 software program. Electronic and geometrical parameters of Ag(I) complexes (**I**–**IV**) are presented in Table 2.

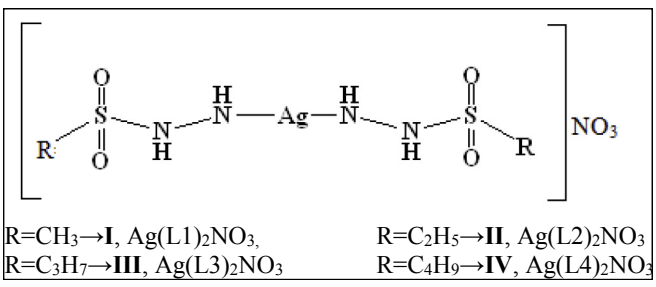

Fig. 2. The structure of Ag(I) alkyl sulfonic acid hydrazide homologous series (**I**–**IV**).

3.1. Characterization of complexes

3.1.1. FT-IR spectra

The selected vibration frequencies of silver(I) complexes with alkyl sulfonic acide hydrazides are listed in Table 3. In order to clarify bonding sites of ligand to metal ion, IR spectra of metal complexes were studied and assigned based on careful comparison of their spectrum with that of free ligands. NH_2 vibrations consist of asymmetric and symmetric stretching modes; υ_{as} (H–N–H) and υ_{sym}(H–N–H) are observed between 3383 and 3334 cm^{-1} and 3300-3249 cm^{-1} as double bands in the prepared ligands (L**1-L4**), respectively [18,39–41]. In silver(I) complexes, these frequencies shift to lower range of 3363-3266 cm^{-1} and 3290-3240 cm^{-1} indicating coordination of ligand through a primary nitrogen atom (**N**H_2) to silver(I) ion. Additionally, the presence of a single bands observed about 3210 cm^{-1} and 3211 cm^{-1} confirm the presence of secondary amine groups (NHs) for ligands. In the spectra of complex, the position of these bands remains largely unchanged, suggesting that the seconder NH group of ligands are not involved in coordination to the metal [42]. The IR spectrum of complexes also show bands in 1321–1317 cm^{-1} region attributed to $\nu_{as}(SO_2)$ vibrations and the bands in 1156–1133 cm^{-1} region attributed to the $\nu_{sym}(SO_2)$ vibrations. Compared with ligands, there are no significant changes in these bands [43]. The sulfonyl oxygens do not participate in the coordination and this is not surprising since the examples of coordinated sulfonyl groups are very rare [44]. New bands appeared at lower frequencies in the spectrum of complexes are probably due to metal-nitrogen bonds. The very strong bands corresponding to NO_3^- stretching of uncoordinated nitrate anions are observed between 1370 and 1375 cm^{-1} [45].

3.1.2. LC-MS spectra

The electron impact mass spectrum of the Ag(I) complexes were recorded at 70 eV. The mass spectrum of $[Ag(L)_2]NO_3$ complexes are presented in Fig. 3 and the fragmentation peaks are given in Table 4. LC-MS spectra shows that the molecular ion peaks, $[M]^+$ at *m/z* 327.94 (23%) for $Ag(L1)_2^+$ (complex **I**), $[M]^+$ at *m/z* 355.0(7%) for $Ag(L2)_2^+$ (complex **II**), $[M\text{-}2H]^+$ at *m/z* 381.0(16%) for $Ag(L3)_2^+$ (complex **III**) and $[M + NH_4\text{–}2H]^+$ at *m/z* 427.4 (%10) for $Ag(L4)_2^+$ (complex **IV**). The main peaks (100%), $[M\text{-}2(SO_2\text{–}CH_3)\text{+}Na]^+$ at *m/z* 188.95, $[2L2\text{+}Na]^+$ at *m/z* 273, $[Ag + L3\text{-}2H]^+$ at *m/z* 243.08 and $[L4\text{-}C_2H_5]^+$ at *m/z* 123.04 are observed for $[Ag(L1)_2]NO_3$ (complex **I**), $[Ag(L2)_2]NO_3$ (complex **II**), $[Ag(L3)_2NO_3]$ (complex **III**), $[Ag(L4)_2\text{-}NO_3]$ (complex **IV**), respectively.

Table 2
Selected geometrical and electronic parameters of silver(I) complexes.

Geometrical parameters				Electronic parameters	
Bond length (Å)		Bond angle (°)		FMOs (eV)	
complex I					
Ag25–N11	2.197	N11–Ag25–N14	155.4	LUMO+2	−0.0868
N4–N11	1.480	N4–N11–Ag25	101.8	LUMO+1	−0.1127
S6–N4	2.113	S6–N4–N11	104.4	LUMO	−0.1544
C1–S6	1.946	C1–S6–N4	96.3	HOMO	−0.2056
				HOMO-1	−0.2234
				HOMO-2	−0.2056
complex II					
N10–Ag23	2.203	N10–Ag23–N13	158.0	LUMO+2	−0.0890
N3–N10	1.489	N3–N10–Ag23	111.2	LUMO+1	−0.1129
S5–N3	2.068	S5–N3–N10	105.9	LUMO	−0.1367
C1–S5	1.988	C1–S5–N3	101.9	HOMO	−0.1990
C32–C1	1.560	C32–C1–S5	108.9	HOMO-1	−0.2167
				HOMO-2	−0.2322
complex III					
N10–Ag23	2.202	N10–Ag23–N13	158.2	LUMO+2	−0.0361
N3–N10	1.490	N3–N10–Ag23	111.8	LUMO+1	−0.0561
S5–N3	2.075	S5– N3–N10	105.4	LUMO	−0.0624
C1–S5	1.984	C1–S5–N3	102.6	HOMO	−0.1791
C31–C1	1.560	C31–C1–S5	109.9	HOMO-1	−0.1990
C34–C31	1.593	C34–C31–C1	107.8	HOMO-2	−0.2232
complex IV					
N10–Ag23	2.187	N10–Ag23–N13	167.2	LUMO+2	−0.0335
N3–N10	1.510	N3–N10–Ag23	107.9	LUMO+1	−0.0535
N3–S5	2.040	S5–N3–N10	104.8	LUMO	−0.0598
C1–S5	1.979	C1–S5–N3	101.5	HOMO	−0.1765
C31–C1	1.559	C31–C1–S5	109.6	HOMO-1	−0.1964
C34–C31	1.594	C34–C31–C1	108.5	HOMO-2	−0.2203
C40–C34	1.585	C40–C34–C31	109.9		

3.1.3. Conductivity and magnetic behavior

The electrical molar conductivity (Λ_M, $ohm^{-1}.\ cm^2.mol^{-1}$) values of complexes reach the ranges characteristic for 1:1 electrolyte type comparing with KI (1:1 electrolyte type) as reference and experimental results are presented in Table 5. Ag(I) complexes were characterized by elemental analysis and mass spectrometry methods to confirm the proposed molecular formulas. The electrical molar conductances in methanol at room temperature for $Ag(L)_2NO_3$ were measured in the range of 31.23–32.06 $\Omega^{-1}\ cm^2\ mol^{-1}$ which indicates 1:1 ionic nature of silver (I) complexes and the number of ionized nitrate ions. The measured values are displayed similar to the reference value (1:1 electrolyte type KI).

The effective magnetic moments (μ_{eff}) of complexes (**I**–**IV**) were measured at room temperature as Bohr Magneton (B.M.). The diamagnetic character of $Ag(L)_2NO_3$ complexes shows the linearity of Ag(I) complexes.

3.2. Theoretical calculations

The computational calculations of Ag(I)-alkyl sulfonic acide hydrazides were carried out using the Becke-3-Lee–Yang–Parr density functional methods [46]. The geometry optimizations of silver(I) complexes having distorted linear geometries were applied to confirm the structure as minimum points in energy by PBEPBE/LanL2DZ/DEF2SV quantum set in Gaussian 09 software program. The calculated geometrical parameters (bond lenghts and bond angles), the frontier molecular orbital (HOMO-2, HOMO-1, HOMO and LUMO, LUMO+1, LUMO+2) energies and molecular electrostatic potential (MEP) mapped surfaces were performed with the same quantum set.

3.2.1. Geometrical parameters

The selected geometrical parameters (bond lenghts and bond angles) were determined using PBEPBE method with LanL2DZ/DEF2SV basis set in the gas phase. The selected geometrical parameters of Ag(I) complexes are listed in Table 2. The Ag–N, N–N, N–S and S–C bond distances lie within calculated range of 2.187–2.203 Å, 1.480–1.510 Å, 2.040–2.113 Å and 1.946–2.068 Å, respectively. The N–Ag–N, N–N–Ag, S–N–N and C–S–N bond

Table 3
Wave number (cm^{-1}) of selected vibration of the silver(I) complexes.

Assign.	I	II	III	IV
$\upsilon_{as}(NH_2)$	3350m	3266s	3335m	3363m
$\upsilon_s(NH_2)$	3276m	3241s	3290m	3240m
υ(NH)	3215	3205s	3210	3214w
$\upsilon_{as}(SO_2)$	1321s	1321s	1316s	1324s
$\upsilon_s(SO_2)$	1153s	1148s	1143s	1155s
$\delta(NH_2)$	1627m	1627m	1617m	1633m
$\delta(SO_2)$	527s	522m	527w	529
δ(NH)	644m	548m	578w	580

w:weak, m:medium, s:strong.

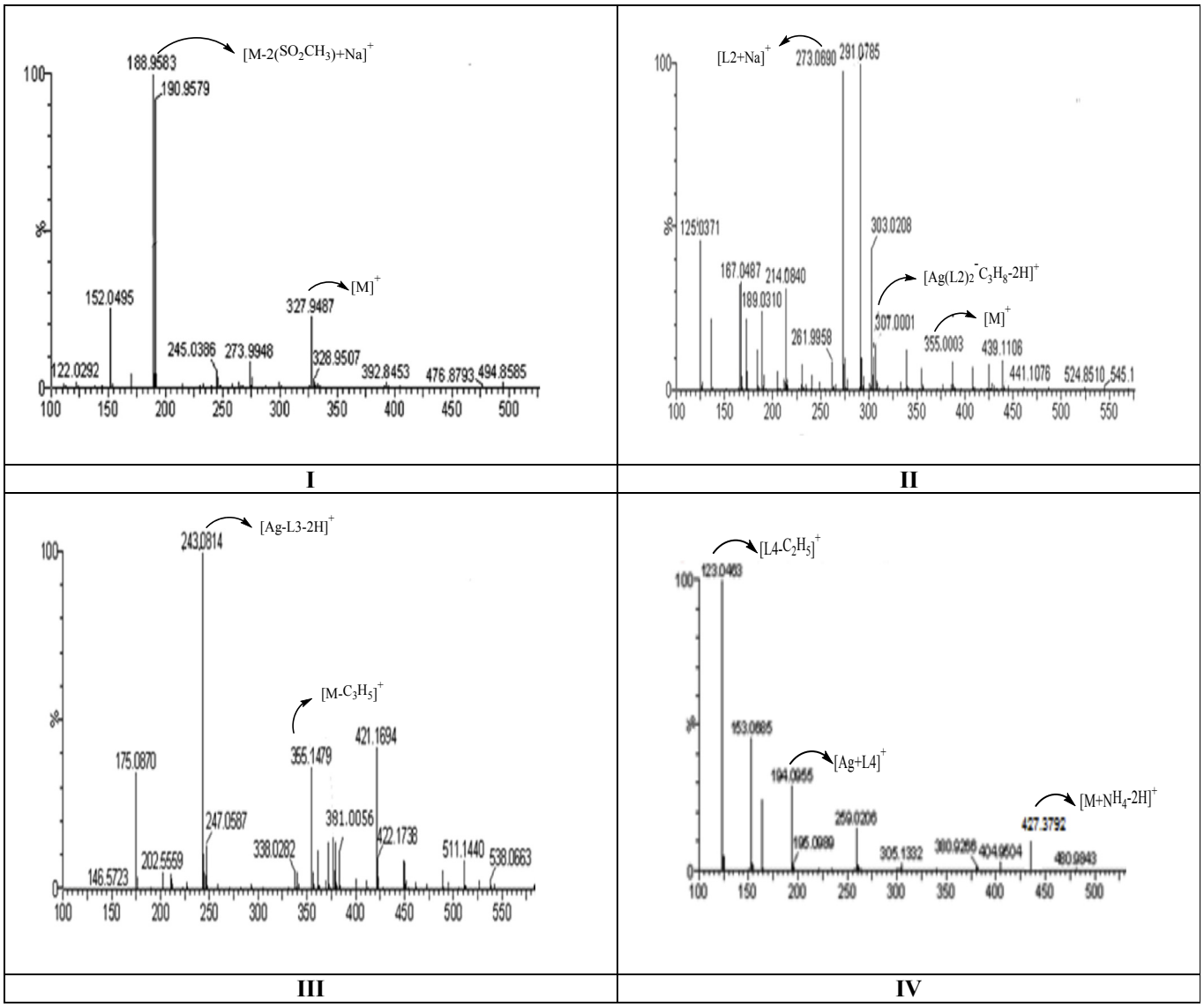

Fig. 3. LC/MS spectrum of silver complexes (**I**–**IV**).

Table 4
The mass spectral data of silver(I) complexes.

Complex	MW	Relative intensities of cationic complexes (m/z, %) and assignment
I	389.87	$[M]^+$ (327.94, %23), $[M\text{-}2(SO_2CH_3)+Na]^+$ (189.95, %100), $[(H_2N–Ag–NH_2–NH)–2H]^+$ (152.05, %25)
II	417.97	$[M]^+$ (355.0, %7), $[Ag(L2)_2\text{-}C_3H_8–2H]^+$ (307.0, %14),$[2L2+Na]^+$ (273, %95), $[Ag + L2\text{-}CH_3\text{-}2H]^+$ (214.08, %31), $[L2+H]^+$ (125.0, %46)
III	445.87	$[M\text{-}2H]^+$ (381.0, %16), $[M\text{-}C_2H_5]^+$ (355.15, %32), $[Ag + L3\text{-}2H]^+$ (243.08, %100)
IV	473.87	$[M + NH_4–2H]^+$ (427.4, %10),$[2L4+Na]^+$(328.91, %11), $[Ag + L4]^+$ (259.87, %7), $[L4+H]^+$ (153.01, %42),$[L4\text{-}C_2H_5]^+$ (123.04, %100)

Table 5
The molar electric conductivity values of the silver complexes (in methanol).

Complex	Λ_M (ohm^{-1} cm^2 mol^{-1})
I	31,23
II	31,46
III	32,06
IV	31,57
KI	31,65

Reference: KI 1×10^{-3} M methanolic solution.

angles were calculated between 155.4 and 167.2°, 101.8–111.8°, 104.4–105.9° and 102.6–102.6°, that shows the distorted linear geometries of silver(I) complexes.

3.2.2. Frontier molecular orbitals (FMOs)

Frontier Molecular Orbital (FMO) surfaces present the various stable electronic distributions of molecules and play an important role in electronic and optical properties. According to FMOs theory, the highest occupied and lowest unoccupied molecular orbitals (HOMOs and LUMOs) are crucial in predicting the chemical reactivities of the species [33,47]. HOMOs and LUMOs are the main

orbitals taking part in the chemical reactions. HOMOs are electron donors representing the ability to donate an electron and LUMOs are electron acceptors representing the ability to obtain an electron. The HOMO energy levels are directly related to the ionization potentials and LUMO energy levels are directly related to the electron affinities.

The HOMOs (HOMO-2, HOMO-1, HOMO) and LUMOs (LUMO, LUMO+1, LUMO+2) energies were calculated by using PBEPBE method with LanL2DZ/DEF2SV basis set [48–51] and FMO surfaces of optimized geometries are exhibited in Fig. 4. The frontier molecular orbital (HOMO and LUMO) energies of silver complexes (**I**–**IV**) are determined between (−0.1765)-(-0.2056) eV and (−0.0598)-(-0.1544) eV, respectively. The lower negative HOMO and LUMO energies indicate that silver(I) complexes may play significant role for drug metabolism as oxidant and reductant. The energy values of other HOMO and LUMO levels are listed in Table 2.

3.2.3. *Molecular electrostatic potential (MEP)*

The molecular electrostatic potential (MEP) shape is a plot of electrostatic potential mapped onto the constant electronic densities which provides information about charge density distributions, chemically active sites and electrophilic interactions in biologic systems The positive electrostatic potential surfaces coloured in shades of blue are correspond to repulsion of the proton by atomic nuclei in the region of lower electron density surfaces. And also, the negative electrostatic potential surfaces coloured in shades of red are correspond to attraction of the proton by the electronic densities in the molecule. The positive regions may be regarded as electrophilic centers whereas the negative regions are considered as nucleophilic sites [52–54]. The electrostatic potentials increase in the order of coloured regions as red < orange < yellow < green < blue.

As reported by Stams at al., MEP analysis of sulfonamides as CA II inhibitors reveals that the negative potential is concentrated on the oxygen of the sulfon moiety which is preferred sites for electrophilic attack, whereas a positive potential indicating the site for nucleophilic attack is concentrated on the NH and NH_2 groups of sulfonamides. The inhibitor coordinates to zinc center of CA II enzyme and sulfonamide nitrogen donates a hydrogen bond to the hydroxyl group of Thr-199. Sulfonyl oxygen accepts a hydrogen bond from the backbone amide NH of Thr-199 and NH_2 of Gln-92. However, Thr-200 accepts a hydrogen bond from nitrogen of the inhibitor [55].

The molecular electrostatic potentials (MEPs) of the optimized Ag(I) complexes with atomic numbering were determined by using PBEPBE/LanL2DZ/DEF2SV quantum set with DFT method. As seen in Fig. 5, the regions of the negative potential (reddish) are over SO_2 and NO_3^- groups, besides regions of the positive potential (bluish) are over NH_2 and NH groups. The molecular electrostatic potential (MEP) mapped surfaces may be employed to understand the reactive sites of Ag(I)-alkyl sulfonic acide hydrazide complexes for the interaction with biological molecules [18,55].

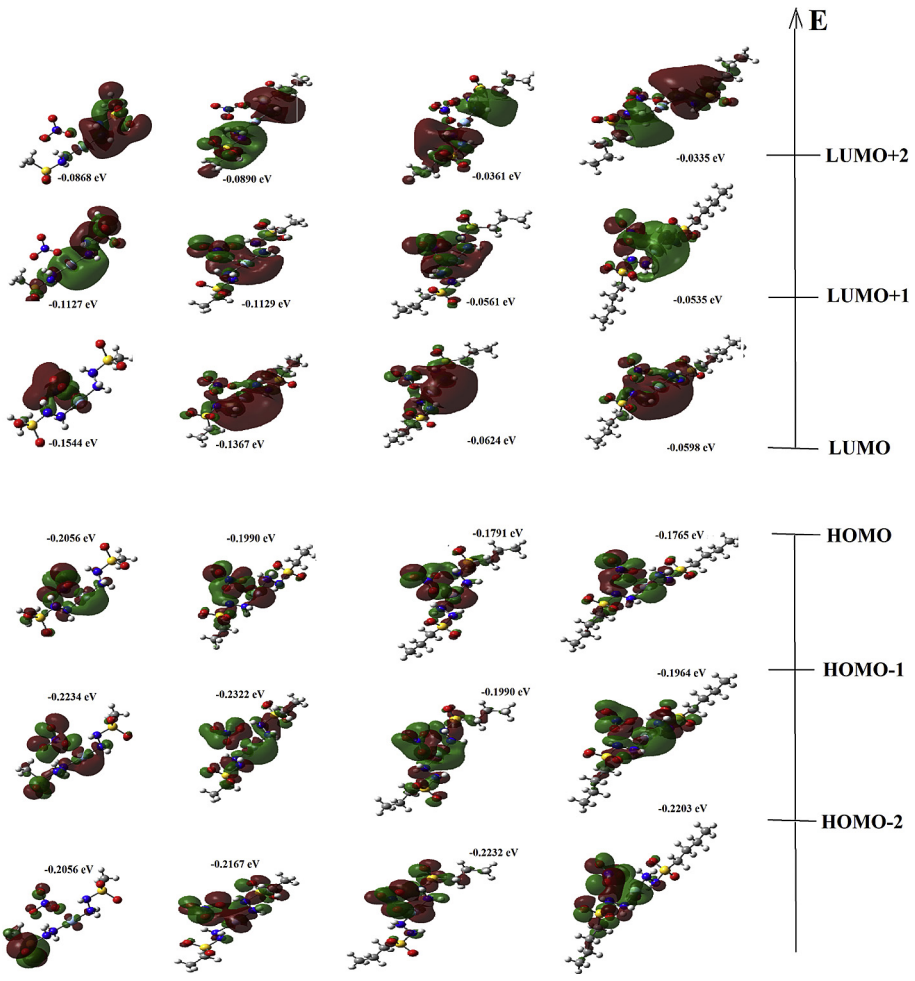

Fig. 4. Frontier molecular orbitals (HOMOs and LUMOs) of complexes (**I**–**IV**).

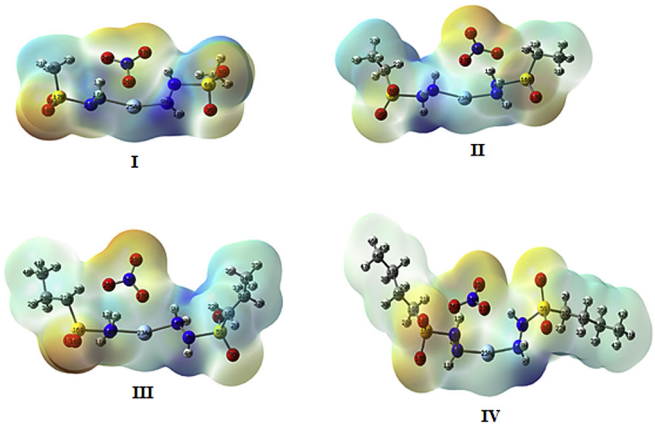

Fig. 5. The molecular electrostatic potential (MEP) mapped surfaces of optimized complexes (**I**–**IV**).

Table 6
Cytotoxicities of silver(I) complexes (**I-IV**) and Docetaxel against MCF-7 cell lines.

Compound	IC_{50} ($\mu molL^{-1}$)
I	11.6 ± 0.5
II	8.12 ± 1.1
III	6.9 ± 0.8
IV	5.10 ± 1.0
Docetaxel	7.24 ± 0.8

Reference: Docetaxel as standard drug.

3.3. Biological studies

3.3.1. In vitro antitumor activities

The inhibitory effects of silver complexes (**I**–**IV)** were treated on human breast cancer, MCF-7 cells and the growth of cells were examined with MTT assay method. The cytotoxic activities as 50% inhibitory concentration (IC_{50}) values are shown in Table 6. The in vitro cytotoxicity of silver complexes (**I**–**IV)** against MCF-7 cell lines were investigated and compared with Docetaxel, the drug used as standard. It can be seen that, the IC_{50} values of complex **III** (6.9 ± 0.8 μM) and complex **IV** (5.10 ± 1.0 μM) against MCF-7 lower than Docetaxel (7.24 ± 0.8 μM). Upon comparing the activities of the reported complexes, **IV** shows higher cytotoxicity against MCF-7, but **I** and **II** have lower potencies (average IC_{50} values of 11.6 ± 0.5 μM and 8.12 ± 1.1 μM) than **III** and **IV** having more methyl units. Viewing from the structure of synthesized silver(I) complexes, it can be assumed that the increasing alkyl units up to 4 (methane, ethane, propane and butane) causes enhance activities in our homolog series.

3.3.2. Antibacterial activity results

The test compounds were screened in vitro for their antibacterial activities against four Gram positive species (*S. aureus, B. subtilis B. cereus* and *E. faecalis*) and three Gram negative species (*E. Coli, P. Aeruginosa* and *K. pneumonia*) by the disc diffusion method and inhibition zones of complexes (**I**–**IV**) are presented in Table 7. The activity results were compared with those of the standard antibiotics as sulfamethoxazole and sulfisoxazole. The size of the inhibition zone depends upon the culture medium, incubation conditions, rate of diffusion and the concentration of the antibacterial agent (the activity increases as the concentration increases). In the present study, the silver(I) complexes with alkylsulfonic acide hydrazides are active against both types of the Gram positive and Gram negative bacteria.

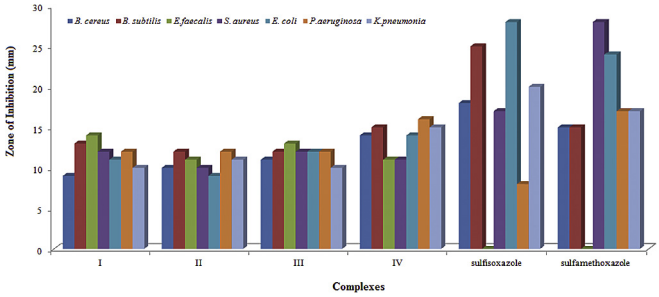

Fig. 6. Comparison of antibacterial activities of complexes (**I**–**IV**) and antibiotics.

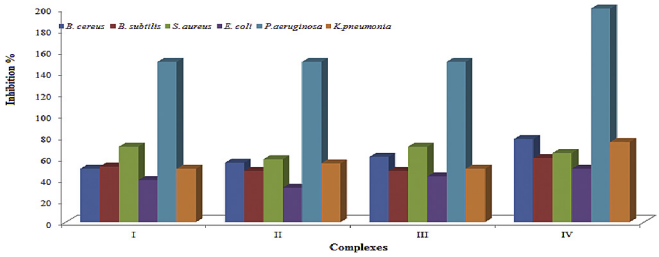

Fig. 7. Percentage of inhibition of complexes (**I**–**IV)** against sulfisoxazole.

As the disc diffusion assay results evidently show that complex **IV** with longest alkyl chain exhibits generally strong inhibition effects against tested bacteria whereas the other complexes (**I**–**III)** have moderate activities as seen in Fig. 6. The silver(I) complexes with alkyl sulfonic acide hydrazides show the highest activities against *E. Faecalis* in the diameter zone of 11–14 mm whereas sulfisoxazole and sulfamethaxazole, the drug used as standard, have been found inactive. This result is interesting that the silver complexes (**I**–**IV)** have much more selectivities against *E. Faecalis* than free ligands [18]. Akgül et al. determined antibacterial activities of synthesized sulfonamide derivatives and standard antibiotics (Gentamisin and Co-trimoxazole) as positive control. The screening test was performed by using disc diffusion method for detecting the susceptibility of synthesized compounds and positive

Table 7
Inhibition zone values (mm, 100 μg/disc) of the silver complexes by disc diffusion method.

Compound	Gram positive				Gram negative		
	B.subtilis RSKK 244	*B. cereus NRRL-B*-3711	*E. faecalis ATCC* 29212	*S. aureus ATCC* 25923	*P.aeruginosa ATCC* 15442	*K.pneuonia ATCC* 70063	*E. coli ATCC* 11230
I	13	9	14	12	12	10	11
II	12	10	11	10	12	11	9
III	12	11	13	12	12	10	12
IV	15	14	11	11	16	15	14
Sulfisoxazole	25	18	–	17	8	20	28
Sulfamethaxazole	15	15	–	18	17	17	24

References: Sulfisoxazole and Sulfamethaxazole as standard antibiotics.

Table 8
The results of esterase activities on carbonic anhydrase II (hCA II).

Compound	IC_{50} (M)	Ki (M)
I	$2,44 \times 10^{-4}$	$1,88 \times 10^{-4}$
II	$2,27 \times 10^{-4}$	$1,75 \times 10^{-4}$
III	$2,07 \times 10^{-4}$	$1,59 \times 10^{-4}$
IV	$1,91 \times 10^{-4}$	$1,47 \times 10^{-4}$
AAZ	1.13×10^{-4}	$2,11.10^{-5}$

Reference: AAZ (Acetazolamide) as standard inhibitor.

controls to *E. faecalis* ATCC 29212. The antibacterial activities of Gentamisin and Co-trimoxazole as positive control were found about 13 mm and 31 mm, respectively. Our silver(I) complexes have similar activities with Gentamisin, but have lower activities than Co-trimoxazole [56].

Percentage of inhibition for the compounds is exhibited in Fig. 7 that is expressed as excellent activity (120–200% inhibition), good activity (90–100% inhibition), moderate activity (75–85% inhibition), significant activity (50–60% inhibition), negligible activity (20–30% inhibition) and no activity. As seen in Fig. 7, all of the complexes (**I**–**IV**) (160–200%) show excellent activity against bacteria *P. aeruginosa* (Sulfisoxazole is accepted 100% inhibition). Especially, complex **IV** (200%) has the best activity against bacteria *P. aeruginosa.*

The results obtained by the disc diffusion method indicates that the number of carbon atoms in alkyl sulfonic acide hydrazide coordinated to silver ion may play an important role in the antibacterial activities. The highest antibacterial activity was observed for complex **IV** which has alkyl sulfonic acide hydrazide with an aliphatic carbon chain of 4 carbon atoms.

3.3.3. *hCA II enzyme inhibition results*

The object of this study is to determine the inhibitory effects of the silver(I) complexes against hCA II isoenzyme. The inhibitory effects of newly synthesized Ag(I) complexes were evaluated by using IC_{50} (IC_{50} represents the molarity of inhibition as 50% decrease of enzyme activity) and K_i (inhibitor–enzyme dissociation constant) values which are two of the most appropriate parameters of the inhibitors (Table 8) [25]. Acetazolamide (5-acetamido-1,3,4-thiadiazole-2-sulfonamide, AAZ) has also been investigated as standard inhibitor, clinically used against hCA II. As seen in Fig. 8, Ag(I) complexes behave as inhibitors against hCA II, however complex **IV** has the higest inhibitor effect ($K_i = 1,47 \times 10^{-4}$ M, $IC_{50} = 1,91 \times 10^{-4}$ M) than the other complexes (**I-III**) on hCA II isoenzyme. Ki and IC_{50} values of complex **IV** are very close to reference drug's. This is probably due to the further effect of the length of an alkyl chain in the tested compounds. Alkyl groups with different R-groups are very often investigated during the drug discovery. Analog series are made by repeatedly adding an extra carbon to alkyl chain and called homologues. If the homologues have a longer and longer chain with no branching, they are called homologous series. Within the homologous series, biological activity often increases to a maximum as a side chain is lengthened. This behavior is often seen in both biochemical and cell-based analysis. Increasing the length of alkyl chain changes the lipophilicity thus causes easily crossing through the cell membrane. In many of the homologous series, the lipophilicities have optimal values. If lipophilicity is too low, the compound hardly crosses the membranes and if the lipophilicity is too high, the compound enters the membrane easily. Tested homologous series can help discovery of the suitable lipophilic properties. This activity trend has less to do with target binding which can be determined in the biochemical assay methods [18,57].

4. Conclusions

In this study, we report the synthesis of silver complexes of alkyl sulfonic acide hydrazides. The structural characterizations of Ag(I) complexes were made by using the elemental analysis and

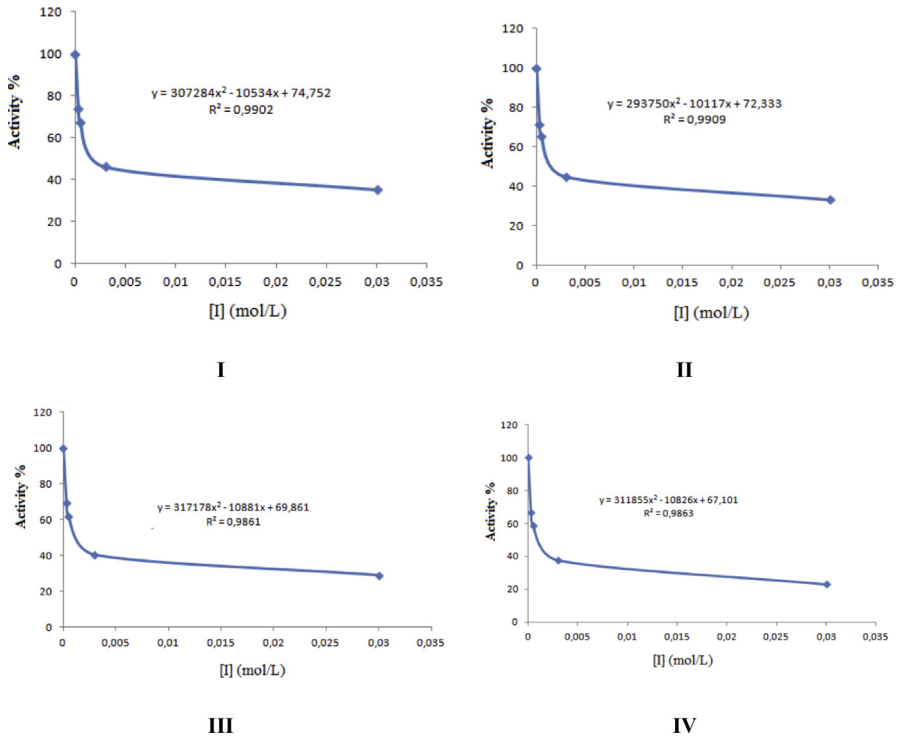

Fig. 8. Activity% vs [I] regression analysis graphs for silver(I) complexes (**I**–**IV**).

spectroscopic methods. Based on physicochemical evidence, the proposed structure of Ag(I) complexes (**I**–**IV**) are exhibited in Fig. 2. Diamagnetic Ag(I) complexes indicating distorted linear geometry were optimized by using PBEPBE method with LanL2DZ/DEF2SV theory level. Geometrical parameters (bond length and bond angles) and electronic properties (HOMO-LUMO energies and MEP mapped surfaces) were also determined with the same basis set. The energies of the frontier orbitals (HOMOs and LUMOs) are important properties in chemical and pharmacological processes giving information on the electron donating and accepting characters of the compounds.

One of the most interesting approach of quantum chemical investigations is to explain the reactivity of compounds. In term of reactivity, electrostatic potential also plays an important role fort he explanation of the reactivity. The reactivity of chemical systems can be evaluated by predicting electrophilic as well as nucleophilic sites in target molecules [58]. MEP analysis of all silver(I) complexes (**I**–**IV**) reveals that the negative potentials are concentrated on the oxygen of the sulfon moieties which are preferred sites for electrophilic attack with biological molecules, whereas a positive potential indicating the site for nucleophilic attack is concentrated on the NH_2 and NH group of Ag(I) complexes. The remarkable activity of complex **IV** may be arising from increasing methyl units which may play an important role in biological activities [57]. Changing the alkyl chain increases the lipophilicity and provides easily passes through the cell membrane. Ag(I) complex (**IV**) with increasing methyl units show highest inhibition effects against breast cancer cell lines MCF-7 (with IC_{50}: 5.10 ± 1.0 μmol/L, having higher activity than standard drug Docetaxel with IC_{50}: 7.24 ± 0.8), all tested bacteria (with 11–16 mm zone diameter range) and CA II isoenzyme (with IC_{50}:1,91 × 10^{-4} M).

Acknowledgements

This research was supported by Gazi University Research Found under Project No 05/2012-12. We thank Ankara University, Faculty of Pharmacy. Central Labs. for allocation of time at the Mass Spectra and Elemental Analyses.

References

[1] C.G. Hartinger, P.J. Dyson, Chem. Soc. Rev. 38 (2009) 391.
[2] L. Mercs, M. Albrecht, Chem. Soc. Rev. 39 (2010) 1903.
[3] M. Patra, G. Gasser, N. Metzler-Nolte, Dalton Trans. 41 (2012) 6350.
[4] B. Thati, A. Noble, B.S. Creaven, M. Walsh, M. McCann, K. Kavanagh, M. Devereux, D.A. Egan, Cancer Lett. 248 (2007) 321.
[5] C.N. Banti, S.K. Hadjikakou, K. Sotoris, Metallomics 5 (2013) 569.
[6] B. Biersack, A. Ahmad, F.H. Sarkar, R. Schobert, Curr. Med. Chem. 19 (2012) 3949.
[7] C.T. Supuran, A. Casini, A. Mastrolorenzo, A. Scozzafava, Mini Rev Med. Chem. 4 (2004) 625.
[8] S.M.I. Morsy, A.M. Badawi, A. Cecchi, A. Scozzafava, C.T. Supuran, J. Enzyme Inhib. Med. Chem. 24 (2009) 499.
[9] S.M. Marques, E.A. Enyedy, C.T. Supuran, N.I. Krupenk, S.A. Krupenko, Bioorg. Med. Chem. 18 (2010) 5081.
[10] W. deKeizer, M.E. Bienenmann-Ploum, A.A. Bergwerff, W. Haasnoot, Anal. Chim. Acta 620 (2008) 142.
[11] A. Innocenti, A. Maresca, A. Scozzafava, C.T. Supuran, Bioorg. Med. Chem. Lett. 18 (2008) 3938.
[12] K.K. Sahu, V. Ravichandran, V.K. Mourya, R.K. Agrawal, Med. Chem. Res. 15 (2007) 418.
[13] S. Roland, R. Ferone, R.J. Harvey, V.L. Styles, R.W. Morrison, J. Biol. Chem. 254 (1979) 10337.
[14] N.C. Baenziger, A.W. Struss, Inorg. Chem. 15 (1976) 1807.
[15] D.S. Cook, M.F. Turner, J. Chem. Soc. Perkin Trans. 2 (1975) 1021.
[16] N.C. Baenziger, S.L. Modak, C.L. Fox, J. Acta Crystallogr. Sect. C 39 (1983) 1620.
[17] R.A. Khan, K.A. Farhan, A. Almeida, A. Alsalme, A. Casini, M. Ghazzali, J. Reedijk, J. Inorg. Biochem. 140 (2014) 1.
[18] U.O. Ozdemir, F. Ilbiz, A.B. Gunduzalp, N. Ozbek, Z.K. Genç, F. Hamurcu, S. Tekin, J. Mol. Struct. 1100 (2015) 464.
[19] U.O. Ozdemir, N. Akkaya, N. Özbek, Inorg. Chim. Acta 400 (2013) 13.
[20] U. Ozdemir, O.S. Senturk, S. Sert, N. Karacan, F. Uğur, J. Coord. Chem. 59 (2006) 1905.
[21] U. Ozdemir, N. Karacan, O.S. Senturk, S. Sert, F. Uğur, Synt. React Inorg Met Org. Chem. 34 (2004) 1057.
[22] G. Orhan, O.S. Senturk, U.O. Ozdemir, S. Sert, E. Subasi, J. Coord. Chem. 67 (2014) 3216.
[23] O.S. Senturk, S. Sert, U. Ozdemir, Z. Naturforsch 58 (2003) 1124.
[24] O.S. Senturk, U. Ozdemir, S. Sert, N. Karacan, F. Uğur, J. Coord. Chem. 60 (2007) 229.
[25] U. Ozdemir, F. Arslan, F. Hamurcu, Spectrochim. Acta Part A 75 (2010) 121.
[26] U.O. Ozdemir, G. Olgun, Spectrochim. Acta Part A 70 (2008) 641.
[27] U.O. Ozdemir, A. Altuntaş, A.B. Gündüzalp, F. Arslan, F. Hamurcu, Spectrochim. Acta Part A 128 (2014) 452.
[28] S. Alyar, H. Alyar, U.O. Ozdemir, O. Sahin, K. Kaya, N. Ozbek, A.B. Gunduzalp, J. Mol. Struct. 1094 (2015) 237.
[29] N. Özbek, S. Alyar, S. Mamaş, E. Şahin, N. Karacan, J. Mol. Struct. 1010 (2012) 1.
[30] S. Alyar, H. Zengin, N. Özbek, N. Karacan, J. Mol. Struct. 992 (2011) 27.
[31] S.M. Soliman, M.A.M. Abu-Youssef, T.S. Kassem, R. Assem, Spectrochim. Acta Part A 149 (2015) 352.
[32] R.H. Rohrbaugh, P.C. Jurs, Anal. Chim. Acta 199 (1987) 99.
[33] U.O. Ozdemir, E. Aktan, F. Ilbiz, A.B. Gündüzalp, N. Özbek, M. Sarı, Ö. Çelik, S. Saydam, Inorg. Chim. Acta 423 (2014) 194.
[34] F. Denizot, R. Lang, J. Immunol. Methods 89 (1986) 271.
[35] R.B. Mulaudzi, A.R. Ndhlala, M.G. Kulkarni, J.F. Finnie, J. Van Staden, J. Ethnopharmacol. 135 (2011) 330.
[36] J. McD Armstrong, Direcck V. Myers, Jacob A. Verpoorte, John T. Edsall, J. Biol. Chem. 241 (1966) 5137.
[37] S.L. Bradbury, J. Biol. Chem. 244 (1969) 2002.
[38] C. Temperini, A. Scozzafava, L. Puccetti, C.T. Supuran, Biorgan. Med. Chem. Lett. 15 (2005) 5136.
[39] A.B. Gündüzalp, Ü.Ö. Özdemir, B.S. Çevrimli, S. Mamaş, S. Çete, Med. Chem. Res. 23 (2014) 3255.
[40] F. Hamurcu, S. Mamaş, U.O. Ozdemir, A.B. Gündüzalp, O.S. Senturk, J. Mol. Struct. 1118 (2016) 18.
[41] R. Adıgüzel, H. Esener, Z. Ergin, E. Aktan, N. Turan, M. Şekerci, Asian J. Chem. 23 (2011) 2795.
[42] H. Esener, R. Adiguzel, Z. Ergin, E. Aktan, N. Turan, M. Sekerci, Adv. Sci. Lett. 4 (2011) 11.
[43] S. Alyar, N. Ozbek, N. Ocak, Med. Chem. Res. 22 (2013) 2051.
[44] N.I. Dodoff, M. Kubiak, J. Kuduk-Jaworska, Z. Naturforsch 57b (2002) 1174.
[45] D.C. Zhongy, Z.F. Chen, Y.C. Liu, X.J. Luo, C. Barta, H. Liang, J. Coord. Chem. 63 (2010) 3146.
[46] B. Çatıkkaş, E. Aktan, Z. Seferoğlu, Int. J. Quantum Chem. 113 (2013) 683.
[47] A.B. Gündüzalp, G. Parlakgümüş, D. Uzun, Ü.Ö. Özmen, N. Özbek, M. Sarı, T. Tunç, J. Mol. Struct. 1105 (2016) 332.
[48] R.N. Singh, P. Rawat, S. Sahu, J. Mol. Struct. 1065 (2014) 99.
[49] R.N. Singh, V. Baboo, P. Rawat, V.P. Gupta, J. Mol. Struct. 1037 (2013) 338.
[50] A. Srivastava, P. Rawat, P. Tandon, R.N. Singh, Comp. Theo. Chem. 993 (2012) 80.
[51] R.N. Singh, A. Kumar, R.K. Tiwari, P. Rawat, J. Mol. Struct. 1035 (2013) 295.
[52] S. Chidangil, M.K. Shukla, P.C. Mishra, J. Mol. Model 4 (1998) 250.
[53] P. Ekmekcioglu, N. Karabocek, S. Karabocek, M. Emirik, J. Mol. Struct. 1099 (2015) 189.
[54] B. Babür, N. Seferoğlu, E. Aktan, T. Hokelek, E. Şahin, Z. Seferoğlu, J. Mol. Struct. 1081 (2015) 175.
[55] T. Stams, Y. Chen, P.A. Boriack-Sjodin, J.D. Hurt, J. Liao, J.A. May, T. Dean, P. Laipis, D.N. Silverman, D.W. Christianson, Protein Sci. 7 (1998) 556.
[56] Ö. Akgül, İ. Öztürk, A. Aygül, Ş. Ermertcan, Marmara Pharm. J. 21 (2017). XXX.
[57] S. Erland, Mol. Basis Drug Discov. Med. Chem (2014). Chapter 11 Part 3, Alkyl Group Replacements.
[58] M. Noreen, N. Rasool, Y. Gull, M. Zubair, T. Mahmood, K. Ayub, F.H. Nasim, A. Yaqoob, M. Zia-Ul-Haq, V. Feo, Molecules 20 (2015) 19914.